Excited States of Weakly Bound Bosonic Clusters: Discrete Variable Representation and Quantum Monte Carlo†

M. P. Nightingale‡

Department of Physics, East Hall, University of Rhode Island, Kingston, Rhode Island 02881

Pierre-Nicholas Roy*

Department of Chemistry, University of Alberta, Edmonton, Alberta, Canada, T6G 2G2

Received: November 14, 2005; In Final Form: December 28, 2005

We compare two approaches for the accurate calculation of the energy levels of weakly bound boson trimers. The first approach is based on correlation function Monte Carlo employing optimized trial functions, while the second approach is based on the discrete variable representation. A trimer with atoms of half the mass of neon is used as a test problem for benchmark calculations. The two approaches yield identical results, within error bars, for all the $J = 0$ energy levels below the dissociation threshold. The relative merits of the two techniques are discussed, and a perspective is given for extension to larger clusters.

I. Introduction

The study of weakly bound van der Waals clusters is of great current interest. For instance, recent experiments on doped helium clusters have raised fundamental questions regarding superfluidity in finite-size systems.[1,2] For triatomic clusters, the accurate calculation of bound states near and above the isomerization threshold, and up to the dissociation threshold is a current challenge, as is finding an answer to the question how many excited states small ^{4}He clusters have. The latter is important for the interpretation of diffraction experiments on small ^{4}He clusters.[3] These are just a few examples to illustrate the importance of the development of approaches for such calculations.

A standard method is the use of a product-type basis set representation to obtain essentially exact solutions to the Schrödinger equation.[4,5] The solution of the eigenvalue problem can be achieved using iterative procedures such as the Lanczos recursion techniques.[6] The discrete variable representation (DVR) pioneered by Light and co-workers[4,7,8] has been used successfully in this context.

Another very promising method relies the use of many-parameter trial functions which are optimized by means of Monte Carlo (MC) methods. The residual variational bias is subsequently reduced by a correlation function Monte Carlo (CFMC) projection approach.[9,10] More explicitly, the optimization yields a highly correlated, compact basis set for which overlap and Hamiltonian matrix elements are obtained by means of a quantum Monte Carlo imaginary-time projection method which generates results for a sequence of projection times. This is followed by explicit diagonalization to obtain the desired bound-state energies of the cluster.

A more detailed description of the trial states has been given, e.g., in refs 10, 11, and 19. For completeness we mention here that the trial functions have parts that impose short- and long-range boundary conditions; without these, there would be no quantization of energy levels. In addition, the trial wave functions have many variational parameters to describe the correlations in regions in which the cluster is to be found with high probability.

We note that early comparison of the CFMC method to DVR was unfavorable due to convergence problems in DVR.[11] Recent work on neon and argon trimers[12] showed that CFMC and converged DVR results are in excellent agreement. One objective of the present work is to compare the DVR and CFMC approaches for the more weakly bound "half-neon" trimer.

This system will have a higher zero-point energy than the previously studied neon trimer and is expected to provide a more stringent test of the performance of the DVR and CFMC techniques. The present excited-state results also complement a recent study that addressed the issue of interdimensional degeneracies for the ground state of the half-neon trimer.[19] We also stress that we present for the first time, a comparison of the DVR and CFMC methods for *all* the $J = 0$ bound states below the dissociation threshold. We therefore consider the present comparison more complete than the previous one.[12]

The rest of this paper is organized as follows: in section II, we present the two approaches used to obtained bosonic trimer bound states and show and discuss results for the so-called "half-neon" system; we conclude the paper and provide a perspective in section III.

II. Theory and Numerical Results

The "half-neon" trimer is used a benchmark system. More specifically, we use a dimensionless Hamiltonian with pair interactions of the Lennard-Jones form, $r^{-12} - 2r^{-6}$, where r is the distance between two particles. One parameter, the reciprocal mass μ^{-1}, is required. This reciprocal mass is related to the physical particle mass m, and Lennard-Jones core radius σ, and well depth ϵ, through the following relation: $\mu^{-1} = \hbar^2/(m\sigma^2\epsilon)$. The reciprocal mass of "half-neon" is set to $\mu^{-1} = 0.01418$ by definition. The parameter μ, the square of the de Boer parameter (apart from a numerical factor), is proportional to the zero-point energy in a spacial region of linear dimension σ expressed in

† Part of the special issue "John C. Light Festschrift".

* Corresponding author. E-mail: pn.roy@ualberta.ca.

‡ E-mail: nightingale@phys.uri.edu.

10.1021/jp056577q CCC: $33.50
Published on Web 02/07/2006

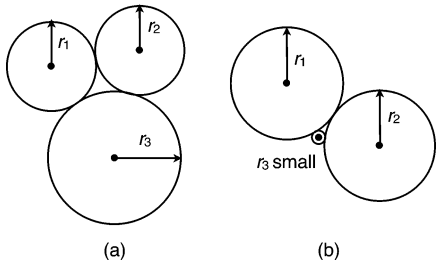

Figure 1. Schematic representation of the Pekeris coordinates, (r_1, r_2, r_3), used in the DVR calculations. The centers of the circle correspond to the positions of the atoms. There exists a unique way to draw three mutually tangent circles, the radii of which define the Pekeris coordinates. (a) When two of the coordinates are equal, $r_1 = r_2$ here, the trimer is in an isosceles configuration. (b) When one coordinate is nearly zero, r_3 is small here, the configuration of the cluster is nearly linear.

units of the well depth ϵ. This parameter is therefore composed of all the factors affecting the floppiness of the system. Using the half-neon value for μ is equivalent to an hypothetical isotopic substitution. This lower reduced mass will yield a smaller number of bound states closer in energy to the continuum of scattering states and with greater delocalization (vide infra). All of these factors contribute to a significant increase of the computational challenge posed by systems of decreased reduced mass.

An important quantity is the dissociation threshold of the cluster. For a trimer, this threshold is defined as the zero-point energy (ground state) of the dimer, E_{20}, where the subscript 2 denotes the two-body nature of the dimer, and the second subscript, 0, denotes the ground state. For the "half-neon" dimer, $E_{20} = -0.427588$.

The two theoretical approaches used in the present work are the MC optimization-CFMC method (CFMC for short) and the Pekeris coordinates DVR method. The CFMC implementation used here is the one described in refs 10 and 11 employing slightly different guiding functions.

The Pekeris coordinates DVR approach of ref 12 is applied here with the following parameters: The dimensionless DVR grid size is ($r_{max} = 5$) and 80 basis functions per degree of freedom are required to obtain the desired accuracy. We set an upper limit (ceiling) of 1000 to the potential. Finally, the basis function parameters are as in ref 12: $a = 3$ $b = 0$. The a parameter has a nonzero value to ensure that the wave function has a nonzero value when the configuration of the trimer is linear, and the b parameter is set to zero to impose bound-state boundary conditions at large interparticle separations. Bound-state energies and wave functions are calculated using the symmetry-adapted Lanczos (SAL) approach.[13,14] An advantage of the Pekeris coordinate system[15,16] is the fact that all degrees of freedom are equivalent and projection operators corresponding to permutation symmetry can be constructed in a straightforward fashion by simple exchange of degrees of freedom. These coordinates do not suffer from the interdependent range problem associated with pair distance coordinates.[17] Finally, the use of Pekeris coordinates allows one to highlight the importance of linear configurations through the analysis of one- and two-dimensional distributions derived from the bound-state wave functions. These qualities have proved useful in the study of structural properties of weakly bound pure[12] and mixed[18] boson trimers. We present in Figure 1 a schematic depiction of the Pekeris coordinates for isosceles and near linear triangular configurations of a trimer.

All "half-neon" trimer bound states with energies below the dissociation threshold, E_{20}, are presented in Table 1. The

TABLE 1: Half-Neon Trimer Bound State Energies Obtained by the CFMC and DVR Methods

		DVR		
k	CFMC	$r_{max} = 3$	$r_{max} = 5$	$r_{max} = 6$
0	−1.308624	−1.308624	−1.308624	−1.308624
1[a]	−0.88032	−0.88032	−0.88032	−0.88032
2	−0.75941	−0.75940	−0.75940	−0.75940
3	−0.56716	−0.56716	−0.56716	−0.56716
4	−0.48046	−0.48038	−0.48054	−0.48054

[a] The statistical error of the CFMC results is estimated to be a few units in the last digit. DVR results for three grid sizes, $r_{max} = 3$, $r_{max} = 5$, and $r_{max} = 6$, are presented. The zero-point energy of the half neon dimer (dissociation threshold) is $E_{20} = -0.427588$. [b] Linear configurations become significant for $k \geq 1$.

agreement between the CFMC and DVR results is excellent. The results are in fact identical for all the digits reported except for states $k = 2$ (0.0013% difference) and $k = 4$ (0.017% difference). These small differences may be explained in terms of statistical errors, but we should note that it can be quite difficult to disentangle these stochastic errors from the systematic bias due to a finite projection time. In the absence of statistical errors the CFMC results would be strict upper bounds to the exact energies. The difference between two calculations is the largest for state $k = 4$. This is the state with the highest energy below the dissociation threshold. Nevertheless, the CFMC result for state $k = 4$ is, as expected based on the variational principle, higher than the exact DVR result. We expect that a longer projection time, which requires a longer Monte Carlo run, or improved trial functions will remove the variational bias and the apparent discrepancy.

We should mention in this context that for the CFMC results it can be quite difficult to decide whether the variational bias has been reduced to below the statisitical error. This is a consequence of the fact that the statistical errors as a function of projection time are correlated, which leads to curves that appear smoother than they would be for uncorrelated errors. In addition, the results are obtained by solving a generalized eigenvalue problem, which features an overlap matrix that is positive definite. The Monte Carlo estimate of this matrix has statistical errors that may destroy this positivity property. With increasing projection time, these errors increase, and the projection process fails dramatically as soon as the computed overlap matrix develops negative eigenvalues. All of these problems tend to produce residual variational bias, i.e., an overestimate of the energy of levels with slower convergence.

We also included in Table 1 DVR results for different values of r_{max} in order to establish convergence. For all states below $k = 4$, a grid size of 3 was sufficient to obtain accurate energies. Results obtained with grid sizes of 5 and 6 are identical.

We present in Figure 2 one-dimensional reduced distribution functions associated with the wave functions. These are obtained by integrating the square of the wave function over all Pekeris coordinates except one.[12] We simply denote this remaining coordinate by r. We first note that for the ground state, the distribution function decays at around $r = 1$, while it was shown in ref 12 that the corresponding distributions decayed at $r = 0.6$ and $r = 0.8$ for the argon and neon trimers, respectively. This additional delocalization of the ground state is a clear indication of the increased floppiness of the half-neon trimer in comparison to the argon and neon cases. The resulting distribution functions will sometimes have a nonzero amplitude at $r = 0$, an indication that linear configuration are possible for a given state. For the half-neon trimer, we see from Figure 2 that all states, except for the ground state ($k = 0$), are likely to

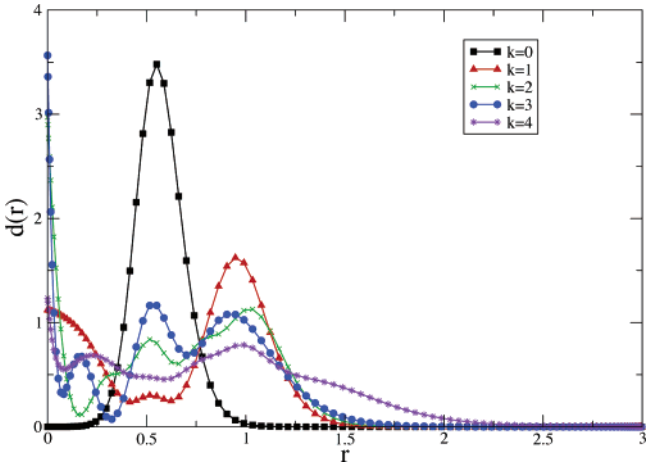

Figure 2. One-dimensional reduced distributions for states $k = 0-4$.

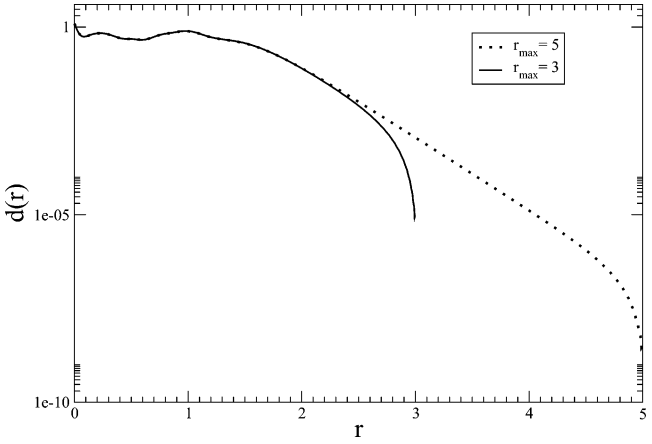

Figure 3. Logarithmic plot of the one-dimensional reduced distribution for the $k = 4$ state for two grid lengths 3 and 5.

have linear configurations. We consider linear configurations to be important when the amplitude at $r = 0$ is of the same order of magnitude as the amplitude at the maximum of the distribution. We have indicated by an asterisk in Table 1 the fact that staring with state $k = 1$, linear configurations become important according to the above definition. For state $k = 4$, the distribution extends to larger values of r. Figure 3 contains a log plot of the one-dimensional reduced distribution function for state $k = 4$ for two grids of length 3 and 5, respectively.

A closer look at the tail of the distribution function for $k = 4$ reveals that the wave function is truncated when a grid size of 3 is used. This incorrect asymptotic behavior can be used to explain why the energy for this shorter grid size is not as negative as the one obtained for a grid size of 5. The agreement between the CFMC and DVR results for $k = 4$ is not as good as in the case of the first four bound states. Maybe this is because the energy of the $k = 4$ state is so close to the dissociation threshold. We finally show in Figure 4 two-dimensional reduced distribution functions[12] for the first five bound states and one state with energy above the dissociation threshold.

This "ink blot" representation reveals the nodal structure of the excited-state wave functions.

III. Conclusions and Outlook

We have shown that the CFMC and DVR methods can yield energy level estimates of comparable accuracy. The "half-neon" trimer was used as a benchmark system because it is more weakly bound than the neon trimer for which the two methods had previously been successfully compared.[12] We have also demonstrated the ability of the CFMC method to calculate *all* the $J = 0$ bound states up to the dissociation threshold. Such a complete comparison of DVR and CFMC had not been presented so far. On the basis of the DVR calculation, we observed that the system contains contributions from linear configurations for all the excited states as revealed by the analysis of distribution functions. The DVR approach allows the calculation of both energy levels and wave functions for ground and excited states whereas the CFMC method have, as far as we know, thus far been used for the calculation of excited energies only. Generalization to the computation of expectation values of operators that are diagonal in the position representation is straightforward in principle, but predicting the accuracy of such an approach is a different matter altogether. The CFMC method can however be applied to much larger problems since it does not suffer from exponential scaling with number of degrees of freedom in contradistiction to product basis methods. This is because the underlying basis functions of the CFMC method are highly correlated multidimensional functions generated by quantum Monte Carlo. Indeed, excited state energies

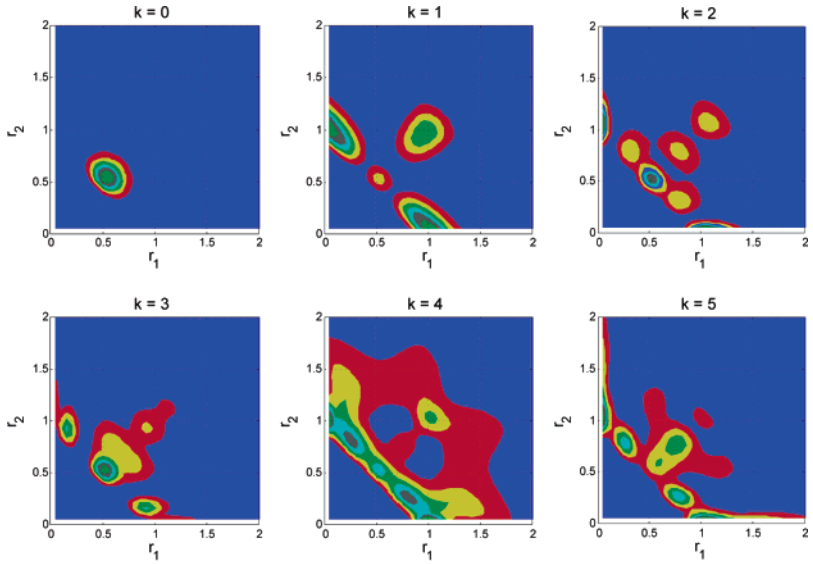

Figure 4. Two-dimensional reduced distributions for the first five bound states and one state above the dissociation threshold.

of seven and five particle systems respectively in three and six spacial dimensions have been obtained with this method.[10,19]

Using DVR type approaches, tetramer calculations are in principle possible now, but pentamer calculations would be intractable with current computers. An important extension of the CFMC method would obviously be the calculation of wave functions. The extension of CFMC method to the case of systems with rigid bonds such as doped helium clusters would be extremely interesting. Here, one could perform the direct calculation of excited states, and therefore transition frequencies that could be compared to recent experiments on He_NOCS and He_NN_2O clusters.[1,2] In these systems, one deals with a rigid molecule with fixed interparticle distances and a floppy helium environment that consists of several atoms. A re-formulation of the CFMC approach in curvilinear coordinates is a possibility for these types of studies. The use of such coordinates would allow one to account for fixed interparticles distances in a straightforward manner. Curvilinear coordinates have recently been used to study the finite temperature properties of various small and medium doped helium clusters.[20−22] If one uses Cartesian coordinates, this constraint has to be accounted for during the Monte Carlo sampling. Techniques used in rigid body quantum Monte Carlo[23−25] could in principle be adapted for the CFMC method for this purpose. With these extensions, the CFMC method could become the approach of choice for the calculation of excited states in weakly bound clusters where the number of degrees of freedom render the use of product-type basis sets impractical.

Acknowledgment. This paper is dedicated to John C. Light. P.-N.R. acknowledges N. Blinov and T. Carrington Jr. for useful discussions. This work was supported by the Natural Sciences and Engineering Research Council of Canada and the Canada Foundation for Innovation and by the United States National Science Foundation under Grant No. ITR 0218858.

References and Notes

(1) Tang, J.; Xu, Y.; McKellar, A. R. W.; Jäger, W. *Science* **2002**, *297*, 2030.
(2) Xu, Y.; Jäger, W.; Tang, J.; McKellar, A. R. W. *Phys. Rev. Lett.* **2003**, *91*, 163401.
(3) Schöllkopf, W.; Toennies, J. P. *J. Chem. Phys.* **1996**, *104*, 1155.
(4) Bacic, Z.; Light, J. C. *Annu. Rev. Phys. Chem.* **1989**, *40*, 469.
(5) Carrington, T., Jr. *Encyclopedia of Computational Chemistry*; Schleyer, P. v. R., Ed.;Wiley: New York, 1998; Vol. 5.
(6) Cullum, J. K.; Willoughby, R. A. *Lanczos Algorithms for Large Symmetric Eigenvalue Computations*; Birkhäuser: Boston, MA, 1985.
(7) Light, J. C.; Hamilton, I. P.; Lill, J. V. *J. Chem. Phys.* **1985**, *82*, 1400.
(8) Light, J.; Carrington, T., Jr. *Adv. Chem. Phys.* **2000**, *114*, 263.
(9) Ceperley, D.; Bernu, B. *J. Chem. Phys.* **1988**, *89*, 6316.
(10) Nightingale, M.; Melik-Alaverdian, V. *Phys. Rev. Lett.* **2001**, *87*, 0434011.
(11) Nightingale, M. P.; Melik-Alaverdian, V. *Recent Advances in Quantum Monte Carlo Methods-Part II*; Lester, W. A., Jr., Rothstein, S. M., Tanaka, S., Eds.; World Scientific: Singapore, 2002; Vol. 2.
(12) Roy, P.-N. *J. Chem. Phys.* **2003**, *119*, 5437.
(13) Wang, X.-G.; Carrington, T., Jr. *J. Chem. Phys.* **2001**, *114*, 1473.
(14) Chen, R.; Guo, H. *J. Chem. Phys.* **2001**, *114*, 1467.
(15) Pekeris, C. L. *Phys. Rev.* **1958**, *112*, 1649.
(16) Davidson, E. R. *J. Am. Chem. Soc.* **1977**, *99*, 397.
(17) Wei, H.; Carrington, T.; Jr. *J. Chem. Phys.* **1994**, *101*, 1343.
(18) Liu, Y. D.; Roy, P.-N. *J. Chem. Phys.* **2004**, *121*, 6282.
(19) Nightingale, M. P.; Moodley, M. *J. Chem. Phys.* **2005**, *123*, 14304.
(20) Blinov, N.; Song, X.-G.; Roy, P.-N. *J. Chem. Phys.* **2004**, *120*, 5916.
(21) Moroni, S.; Blinov, N.; Roy, P.-N. *J. Chem. Phys.* **2004**, *121*, 3577.
(22) Blinov, N.; Roy, P.-N. *J. Low Temp. Phys.* **2005**, *140*, 253.
(23) Buch, V. *J. Chem. Phys.* **1992**, *97*, 726.
(24) Clary, D. C.; Benoit, D. M. *J. Chem. Phys.* **1999**, *111*, 10559.
(25) Sarsa, A.; Schmidt, K. E.; Moskowitz, J. W. *J. Chem. Phys.* **2000**, *113*, 44.